



HAL
open science

Overturning in the Subpolar North Atlantic Program: a new international ocean observing system

M. Susan Lozier, Sheldon Bacon, Amy S. Bower, Stuart A. Cunningham, M. Femke de Jong, Laura de Steur, Brad Deyoung, Juergen Fischer, Stefan F. Gary, Blair J. W. Greenan, et al.

► **To cite this version:**

M. Susan Lozier, Sheldon Bacon, Amy S. Bower, Stuart A. Cunningham, M. Femke de Jong, et al.. Overturning in the Subpolar North Atlantic Program: a new international ocean observing system. Bulletin of the American Meteorological Society, 2017, 98 (4), pp.737-752. 10.1175/BAMS-D-16-0057.1 . hal-04201766

HAL Id: hal-04201766

<https://hal.science/hal-04201766>

Submitted on 15 Sep 2023

HAL is a multi-disciplinary open access archive for the deposit and dissemination of scientific research documents, whether they are published or not. The documents may come from teaching and research institutions in France or abroad, or from public or private research centers.

L'archive ouverte pluridisciplinaire **HAL**, est destinée au dépôt et à la diffusion de documents scientifiques de niveau recherche, publiés ou non, émanant des établissements d'enseignement et de recherche français ou étrangers, des laboratoires publics ou privés.

OVERTURNING IN THE SUBPOLAR NORTH ATLANTIC PROGRAM

A New International Ocean Observing System

M. SUSAN LOZIER, SHELDON BACON, AMY S. BOWER, STUART A. CUNNINGHAM, M. FEMKE DE JONG, LAURA DE STEUR, BRAD DEYOUNG, JÜRGEN FISCHER, STEFAN F. GARY, BLAIR J. W. GREENAN, PATRICK HEIMBACH, NAOMI P. HOLLIDAY, LOÏC HOUPERT, MARK E. INALL, WILLIAM E. JOHNS, HELEN L. JOHNSON, JOHANNES KARSTENSEN, FEILI LI, XIAOPEI LIN, NEILL MACKAY, DAVID P. MARSHALL, HERLÉ MERCIER, PAUL G. MYERS, ROBERT S. PICKART, HELEN R. PILLAR, FIAMMETTA STRANEO, VIRGINIE THIERRY, ROBERT A. WELLER, RICHARD G. WILLIAMS, CHRIS WILSON, JIAYAN YANG, JIAN ZHAO, AND JAN D. ZIKA

A new ocean observing system has been launched in the North Atlantic in order to understand the linkage between the meridional overturning circulation and deep-water formation.

The ocean's meridional overturning circulation (MOC) is a key component of the global climate system (IPCC 2013). The MOC, characterized in the Atlantic (the AMOC) by a northward flux of warm upper-ocean waters and a compensating southward flux of cool deep waters, plays a fundamental role in establishing the mean climate state and its variability on interannual to longer time scales (Buckley and Marshall 2016; Jackson et al. 2015). Coupled with the winter release of locally stored heat, the heat advected northward as part of the upper AMOC limb (Rhines et al. 2008) keeps the Northern Hemisphere generally, and western Europe in particular, warmer than they would be otherwise. Variations in AMOC strength are believed to influence North Atlantic sea surface temperatures (Knight et al. 2005; Delworth et al. 2007; Robson et al. 2012; Yeager et al. 2012), leading to impacts on rainfall over the African Sahel, India, and Brazil; Atlantic hurricane activity; and summer climate

over Europe and North America (Knight et al. 2006; Zhang and Delworth 2006; Sutton and Hodson 2005; Smith et al. 2010). Finally, variability of the inflow of warm Atlantic waters into high latitudes has been linked to the decline of Arctic sea ice (Serreze et al. 2007) and mass loss from the Greenland Ice Sheet (Rignot and Kanagaratnam 2006; Holland et al. 2008; Straneo et al. 2010), both of which have profound consequences for climate variability.

Though less studied than its impact on climate, the AMOC's role in the ocean carbon cycle has emerged as a recent concern. The North Atlantic is a strong sink for atmospheric CO₂ (Takahashi et al. 2009; Khatiwala et al. 2013), accounting for ~40% of the annual mean global air-sea CO₂ flux, with nearly half of that flux occurring north of 50°N. Furthermore, modeling (Halloran et al. 2015; Li et al. 2016) and observational (Sabine et al. 2004) studies show that the North Atlantic plays a crucial role in the uptake of anthropogenic carbon. The

AMOC is believed to play a strong role in creating this carbon sink (Pérez et al. 2013); in addition to transporting anthropogenic carbon northward from the subtropical gyre (Rosón et al. 2003), as these northward-flowing surface waters cool, they absorb additional CO₂ that is carried to depth when deep waters form (Steinfeldt et al. 2009). The carbon flux in the subpolar North Atlantic is also driven by a strong annual cycle of net community production (Kortzinger et al. 2008). AMOC variability can impact this productivity if there is a disruption to the northward flow of nutrients (Palter and Lozier 2008) or to the supply of nutrients to the surface by convection and mixing. Thus, AMOC variability, through its direct impact on CO₂ uptake via transport and overturning and indirectly through its effect on ocean primary productivity, has the potential to alter the ocean's role as a major sink for carbon in the subpolar North Atlantic.

With such a profound array of implications, it is no surprise that a mechanistic understanding of AMOC variability is a high priority for the climate science community. Hypotheses concerning what drives the overturning fall into two categories (Visbeck 2007; Kuhlbrodt et al. 2007): is the AMOC “pushed” by buoyancy forcing at high latitudes, or is it “pulled” by vertical mixing supported by wind and tidal forcing? While both mechanisms contribute to the long-term equilibrium state of the AMOC, it is generally believed that overturning variability on interannual to millennial time scales is linked to changes in buoyancy forcing and to the associated changes in the formation of dense water masses at high latitudes in the North Atlantic. Below, we provide a brief review of that linkage in the modeling and observational context.

Linkage between convection and AMOC variability: Climate models. Current Intergovernmental Panel on Climate Change (IPCC) projections of AMOC slowdown in the twenty-first century based on an ensemble of climate models (see Figs. 12–35 in IPCC 2013) are widely attributed to the inhibition of deep convection at high latitudes in the North Atlantic. Similarly, simulations using twentieth-century coupled ocean–sea ice models also find that AMOC intensification is connected to increased deep-water formation in the subpolar North Atlantic (Danabasoglu et al. 2016). This link between AMOC strength and North Atlantic water mass production was made explicit in a study of climate models where a freshwater anomaly was spread uniformly over the subpolar domain (Stouffer et al. 2006). These “hosing” experiments yielded AMOC decreases, with concomitant decreases in surface air and water temperatures in the high-latitude North Atlantic. However, the adequacy of coarse-resolution models to simulate the ocean's dynamical response to freshwater sources has been called into question in the past few years. For example, Condron and Winsor (2011) argue that the climatic response to anomalous freshwater input needs to be studied with models that resolve the dynamics of narrow coastal flows into and around the North Atlantic basin. Similarly, although a growing number of model simulations suggest that present-day and projected ice loss from the Greenland Ice Sheet may affect the AMOC, the nature and magnitude of the prescribed freshwater fluxes may not appropriately describe how and where Greenland meltwater enters the ocean (Straneo and Heimbach 2013). Clearly, observational studies are needed to guide and constrain modeling efforts aimed at understanding the mechanistic link between convective activity and AMOC variability.

AFFILIATIONS: LOZIER AND LI—Duke University, Durham, North Carolina; BACON AND HOLLIDAY—National Oceanography Centre, Southampton, United Kingdom; BOWER, PICKART, STRANEO, WELLER, YANG, AND ZHAO—Woods Hole Oceanographic Institution, Woods Hole, Massachusetts; CUNNINGHAM, GARY, HOUPERT, AND INALL—Scottish Association for Marine Science, Oban, United Kingdom; DE JONG—Duke University, Durham, North Carolina, and Royal Netherlands Institute for Sea Research, Texel, and Utrecht University, Utrecht, Netherlands; DE STEUR—Royal Netherlands Institute for Sea Research, Texel, and Utrecht University, Utrecht, Netherlands; DEYOUNG—Memorial University, St. John's, Newfoundland, Canada; FISCHER AND KARSTENSEN—GEOMAR Helmholtz Centre for Ocean Research, Kiel, Germany; GREENAN—Bedford Institute of Oceanography, Dartmouth, Nova Scotia, Canada; HEIMBACH—The University of Texas at Austin, Austin, Texas; JOHNS—University of Miami, Miami, Florida; JOHNSON AND MARSHALL—University of Oxford, Oxford, United

Kingdom; LIN—Ocean University of China/Qingdao National Laboratory for Marine Science and Technology, Qingdao, China; MACKAY AND WILSON—National Oceanography Centre, Liverpool, United Kingdom; MERCIER AND THIERRY—CNRS, Laboratory of Ocean Physics and Satellite Oceanography, Ifremer centre de Bretagne, Plouzané, France; MYERS—University of Alberta, Edmonton, Alberta, Canada; PILLAR—Niels Bohr Institute, University of Copenhagen, Copenhagen, Denmark; WILLIAMS—University of Liverpool, Liverpool, United Kingdom; ZIKA—Imperial College London, London, United Kingdom
CORRESPONDING AUTHOR E-MAIL: M. Susan Lozier, mslozier@duke.edu

The abstract for this article can be found in this issue, following the table of contents.

DOI:10.1175/BAMS-D-16-0057.1

In final form 19 August 2016
©2017 American Meteorological Society

Linkage between convection and AMOC variability: Observations. Dense water formation in the Nordic seas and in the North Atlantic subpolar gyre (NASPG) produces the water masses in the AMOC lower limb (Fig. 1). The deepest constituents of the lower limb originate as dense intermediate waters formed in the Nordic seas. These waters, referred to collectively as overflow waters (OW), flow over the shallow sills of the Greenland–Scotland Ridge (GSR) into the North Atlantic: to the east of Iceland is the Iceland–Scotland Overflow (ISO) Water (ISOW), which has traditionally been thought to follow the topography around the Reykjanes Ridge to the Irminger Basin, where it joins the deeper, denser Denmark Strait Overflow (DSO) Water (DSOW). The shallowest component of the AMOC lower limb is the intermediate water produced by deep convection within the NASPG itself. Though this water mass is referred to as Labrador Sea Water (LSW), it is the product of the cumulative transformation of subtropical waters as they flow around the NASPG.

No conclusive observational evidence for a link between dense water formation in the Labrador Sea and AMOC variability has emerged to date (Lozier 2012). The product of that dense water formation—Labrador Sea Water—is exported out of the basin via a deep western boundary current. As such, that boundary current has been closely monitored over the past two decades. Measurements of that boundary current east of the Grand Banks at 43°N during 1993 to 1995 and then again from 1999 to 2001 showed that transport in the LSW density range was remarkably steady despite the fact that LSW production was considerably weaker during the latter period (Clarke et al. 1998; Meinen et al. 2000; Schott et al. 2006; Lazier et al. 2002). Similarly, Dengler et al. (2006) found a strengthening of the deep Labrador Current (LC) at 53°N over the period of a well-documented decrease in convection. Finally, Pickart et al. (1999) showed that, equatorward of the Grand Banks, the deep western boundary current (DWBC) appears weaker when it advects a larger fraction of LSW. As with LSW,

there has been no conclusive observational evidence linking the formation of Nordic seas’ overflow waters with AMOC variability (Jochumsen et al. 2012; Hansen and Østerhus 2007).

One possible reason for the lack for a clear connection between convection and AMOC variability is that not all of the export pathways of dense waters have been monitored. The DWBC has traditionally been considered the sole conduit for the lower limb of the AMOC. However, this assumption has been challenged by observational and modeling studies that reveal the importance of interior, and boundary, pathways (e.g., Bower et al. 2009; Holliday et al. 2009; Stramma et al. 2004; Xu et al. 2010; Lozier et al. 2013).

Second, a direct link between LSW formation and the AMOC has been called into question as more has been learned about the constraints on the spreading of this water away from formation sites (Send and Marshall 1995; Spall and Pickart 2001; Spall 2004; Straneo 2006; Deshayes et al. 2009; Zou and Lozier 2016). Essentially, the compilation of studies over the past decade yields a description of LSW production whereby the properties and transport variability within the DWBC are not a sole function of deep-water formation. Instead, boundary current transport, property gradients between the interior and the boundary current, and the strength of the eddy field all play a role in setting the exit transport and properties. Finally, the linkage between AMOC variability and deep-water formation can be impacted by wind-driven changes in the basin. Since the density

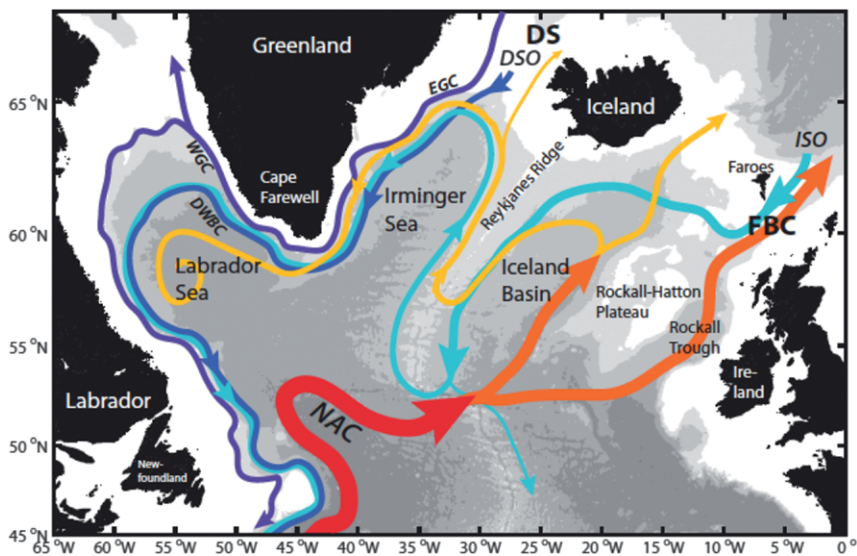


FIG. 1. Schematic of the major warm (red to yellow) and cold (blue to purple) water pathways in the NASPG (credit: H. Furey, Woods Hole Oceanographic Institution): Denmark Strait (DS), Faroe Bank Channel (FBC), East and West Greenland Currents (EGC and WGC, respectively), NAC, DSO, and ISO.

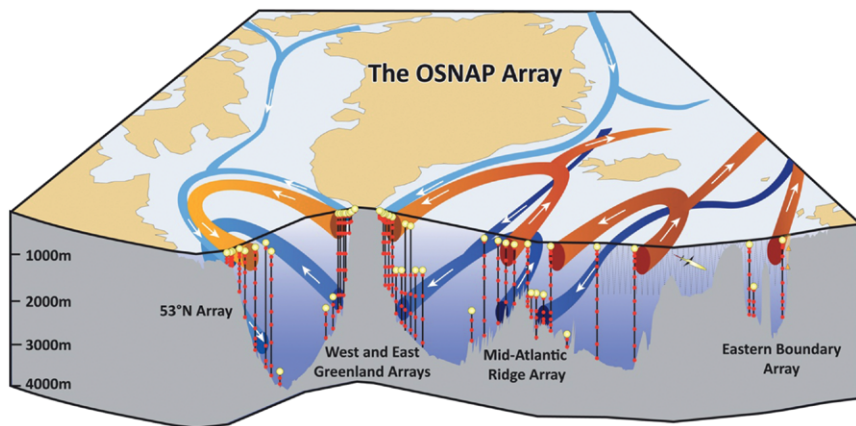


FIG. 2. Schematic of the OSNAP array. The vertical black lines denote the OSNAP moorings with the red dots denoting instrumentation at depth. The thin gray lines indicate the glider survey. The red arrows show pathways for the warm and salty waters of subtropical origin; the light blue arrows show the pathways for the fresh and cold surface waters of polar origin; and the dark blue arrows show the pathways at depth for waters that originate in the high-latitude North Atlantic and Arctic.

forcing in that basin likely offers the best possibility of understanding the mechanisms that underpin AMOC variability. Finally, though it might be expected that the plethora of measurements from the North Atlantic would be sufficient to constrain a measure of the AMOC within the context of an ocean general circulation model, recent studies (Cunningham and Marsh 2010; Karspeck et al. 2015) reveal that there is currently no consensus on the strength or variability of the AMOC in assimilation/reanalysis products.

field near the basin boundaries sets the overall shear of the basinwide geostrophic circulation, wind-forced changes in that density field can modify AMOC strength (Hirschi and Marotzke 2007).

In summary, while modeling studies have suggested a linkage between deep-water mass formation and AMOC variability, observations to date have been spatially or temporally compromised and therefore insufficient either to support or to rule out this connection.

Current observational efforts to assess AMOC variability in the North Atlantic. The U.K.–U.S. Rapid Climate Change–Meridional Overturning Circulation and Heatflux Array (RAPID–MOCHA) program at 26°N successfully measures the AMOC in the subtropical North Atlantic via a transbasin observing system (Cunningham et al. 2007; Kanzow et al. 2007; McCarthy et al. 2015). While this array has fundamentally altered the community’s view of the AMOC, modeling studies over the past few years have suggested that AMOC fluctuations on interannual time scales are coherent only over limited meridional distances. In particular, a break point in coherence may occur at the subpolar–subtropical gyre boundary in the North Atlantic (Bingham et al. 2007; Baehr et al. 2009). Furthermore, a recent modeling study has suggested that the low-frequency variability of the RAPID–MOCHA appears to be an integrated response to buoyancy forcing over the subpolar gyre (Pillar et al. 2016). Thus, a measure of the overturning in the subpolar basin contemporaneous with a measure of the buoyancy

OSNAP OBJECTIVES. Given the imperative of understanding AMOC variability and based on recommendations of the ocean science community (U.S. CLIVAR AMOC Planning Team 2007; Cunningham et al. 2010), an international team of oceanographers has developed an observing system for sustained transbasin measurements in the subpolar North Atlantic, called Overturning in the Subpolar North Atlantic Program (OSNAP). Deployed in the summer of 2014, OSNAP is measuring the full-depth mass fluxes associated with the AMOC as well as meridional heat and freshwater fluxes.

The specific objectives of OSNAP are to:

- 1) quantify the subpolar AMOC and its intra-seasonal to interannual variability via overturning metrics, including associated fluxes of heat and freshwater;
- 2) determine the pathways of overflow waters in the NASPG to investigate the connectivity of the deep boundary current system;
- 3) relate AMOC variability to deep-water mass variability and basin-scale wind forcing;
- 4) determine the nature and degree of the subpolar–subtropical AMOC connectivity; and
- 5) determine from OSNAP observations the configuration of an optimally efficient long-term AMOC monitoring system in the NASPG: such a determination will include the use of numerical model results, satellite altimetry, Argo data, and other NASPG observations as needed.

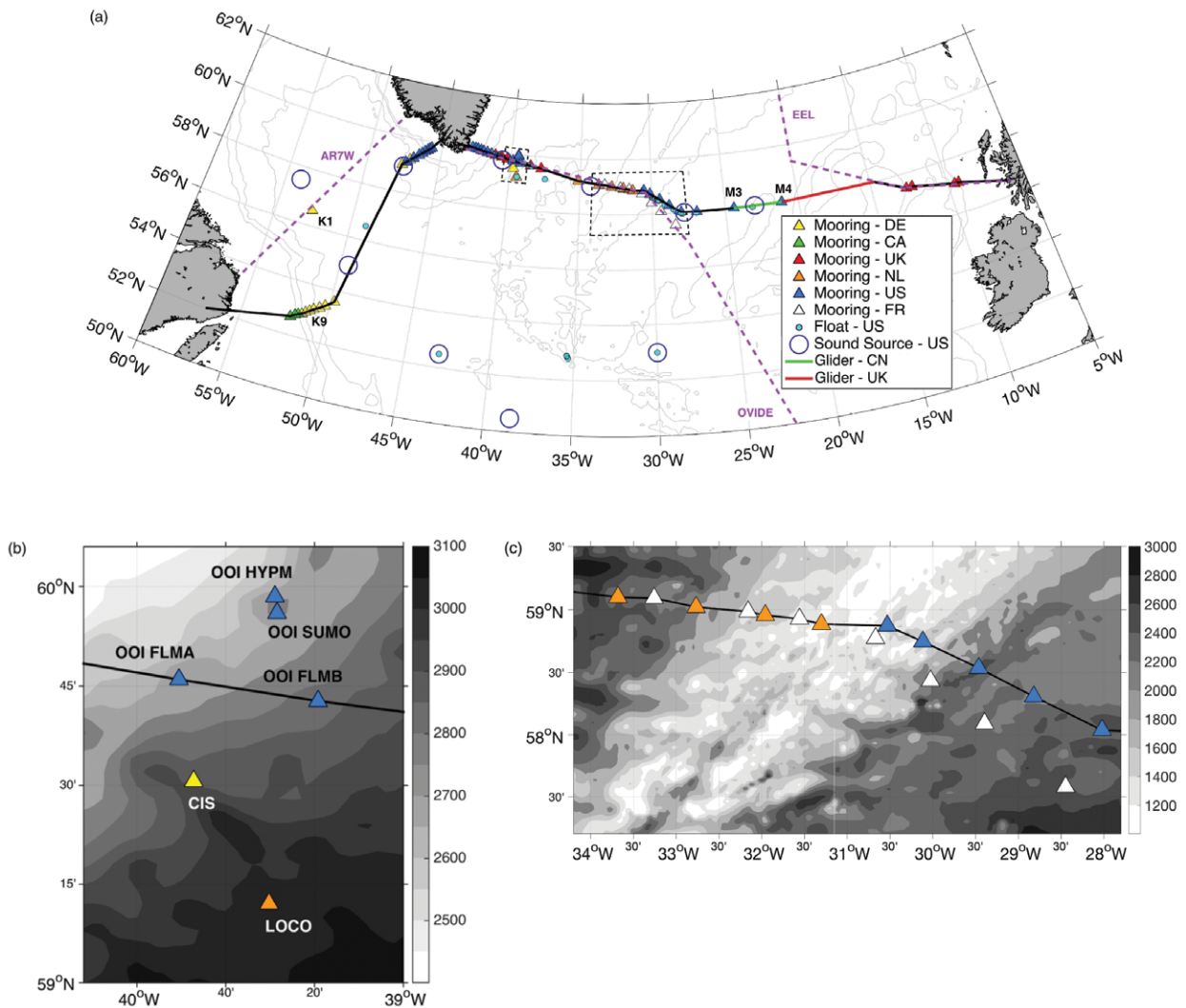


FIG. 3. (a) OSNAP observing system. From west to east, Canadian (CA) shelfbreak array and German (DE) 53°N western boundary array*; U.S. West Greenland boundary array; U.S.–U.K. East Greenland boundary array; Netherlands (NL) western Mid-Atlantic Ridge array; U.S. eastern Mid-Atlantic Ridge array; Chinese (CN) glider survey in the Iceland Basin; U.K. glider survey over the Hatton–Rockall Bank; and U.K. Scottish slope current array. Green dots: 2014 U.S. float launch sites. Green line: Chinese glider; red line: U.K. glider. Blue circles: U.S. sound sources. Purple dashed lines: repeated hydrographic sections. AR7E line is not shown, since it mostly overlaps with the OSNAP East line from Greenland to Scotland. The light gray lines represent the 1,000-, 2,000- and 3,000-m isobaths. Moorings within the black dashed boxes are specified in (b) and (c). (b) OOI Global Irminger Sea array* (blue triangles), which is composed of Apex Surface Mooring (SUMO), Apex Profiler Mooring (HYPM), and Flanking Subsurface Mooring A (FLMA) and B (FLMB); German Central Irminger Sea (CIS) mooring*; and Dutch long-term ocean climate observation (LOCO) mooring*. The OOI FLMA and FLMB are on the OSNAP East line (black line). (c) RREX mooring array* (white triangles) and OSNAP moorings on the flanks of the Reykjanes Ridge. The westernmost three moorings are on the OSNAP East line (black line). In (b) and (c), bathymetry (m) is contoured. An asterisk indicates an observing element that, though used by OSNAP, either existed before OSNAP or came online at the same time. All other elements were designed specifically for OSNAP.

OSNAP DESIGN. OSNAP is a transbasin observing system (Figs. 2 and 3a) that consists of two legs: one leg extends from southern Labrador to southwestern Greenland and the other from southeastern Greenland to the coast of Scotland. The two legs are situated to capitalize on a number of existing long-

term observational efforts in the subpolar North Atlantic: the Canadian Atlantic Repeat Hydrography Line 7 West (AR7W) program in the Labrador Sea (Yashayaev and Loder 2016); the German Labrador Sea western boundary mooring array at 53°N; repeat A1E/AR7E hydrographic sections across the Irminger

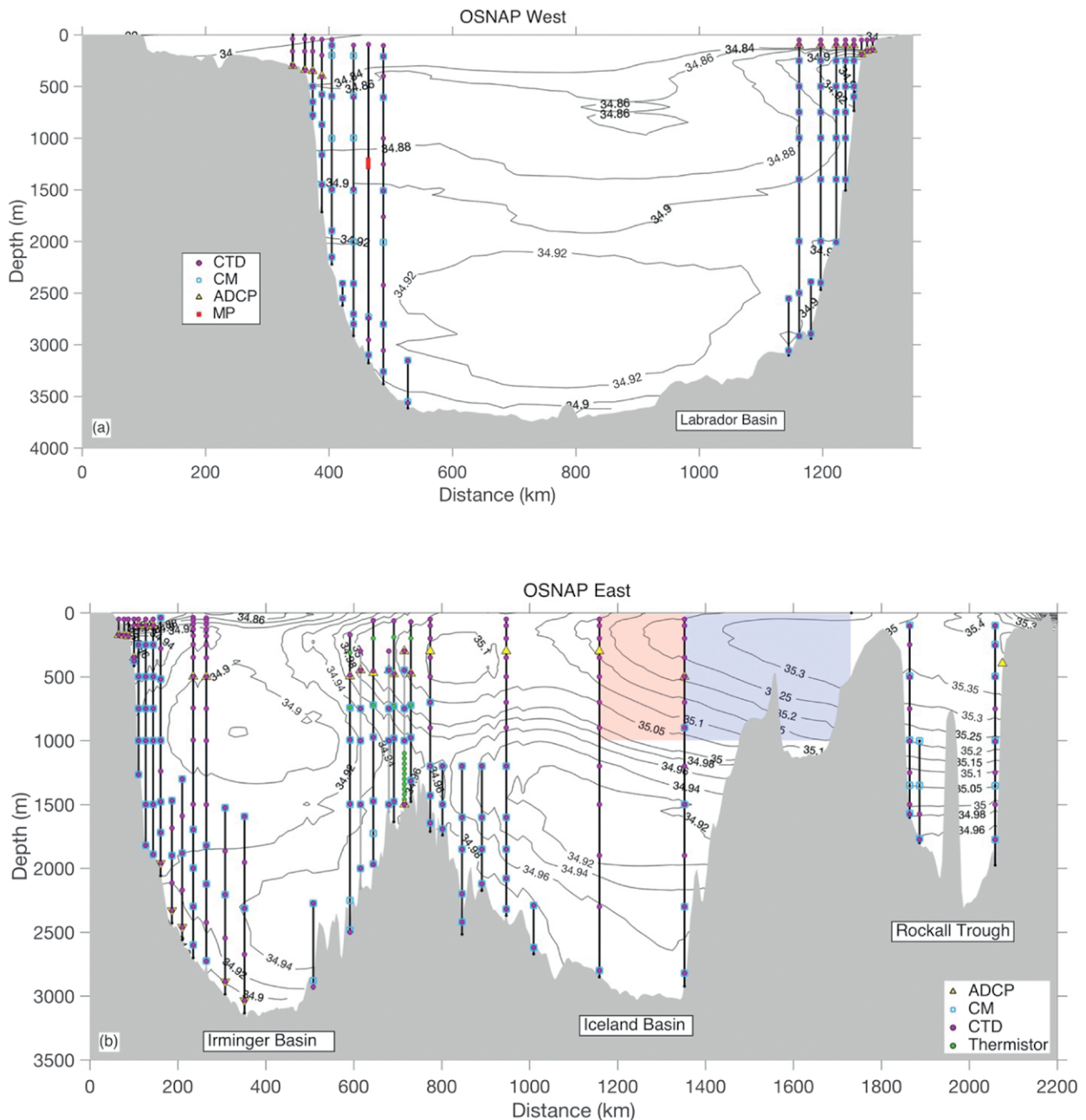


FIG. 4. Schematic of moorings along (a) OSNAP West and (b) OSNAP East. The instrument types are as indicated: thermistor, CTD, current meter (CM), ADCP, and moored profiler (MP). Glider domain is indicated by the shaded box: red: Chinese glider, blue: U.K. glider. Vertical gray lines over the western flank of the Reykjanes Ridge (~600–750 km) along OSNAP East illustrate three French moorings as part of the RREX program. Black contours are 2005–12 mean salinity from *World Ocean Atlas 2013* (Zweng et al. 2013). Enlarged figures are available on the OSNAP website (www.o-snap.org/observations/configuration/).

and Iceland Basins (approximately coincident with OSNAP East); the western part of the biennial Observatoire de la variabilité interannuelle et décennale en Atlantique Nord (OVIDE) line in the Irminger Sea and over the Reykjanes Ridge (Mercier et al. 2015); and the Ellett line (Holliday et al. 2015) in the Rockall region. Importantly, two of the four moorings that

form the U.S. global Ocean Observatories Initiative (OOI) Irminger Sea node were placed along the OSNAP line (Fig. 3b) in August 2014, thereby enhancing the ability of the OSNAP array to capture the full breadth of the deep currents in this basin. OSNAP also complements a new Canadian program in the Labrador Sea [Ventilation Interactions and Transports

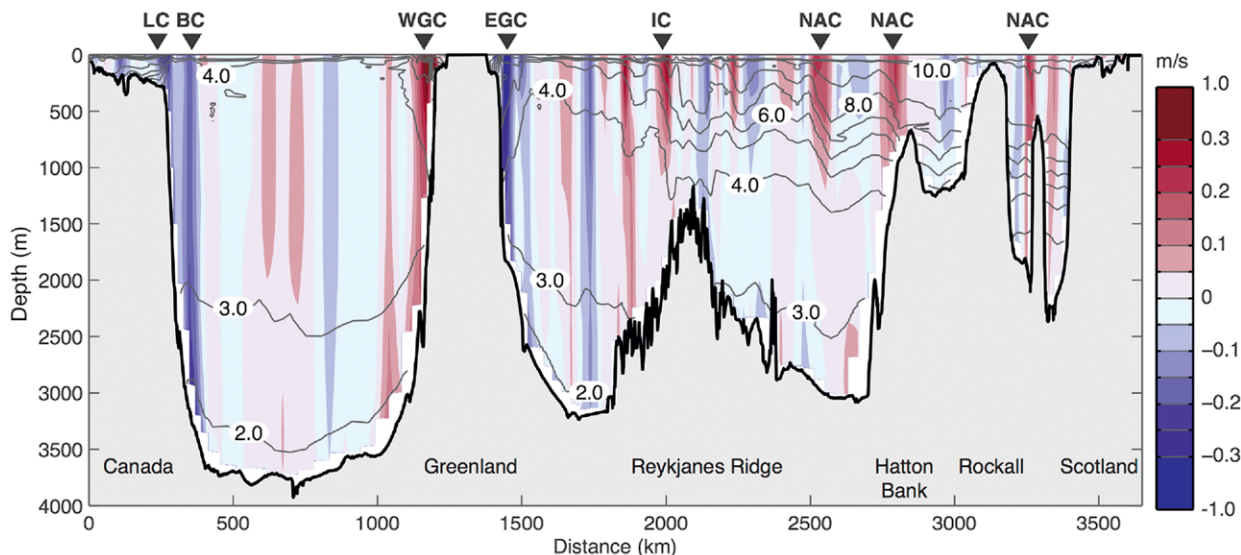


FIG. 5. Observations on the OSNAP section in Jun–Jul 2014; cross-sectional velocity in color (positive is poleward, m s^{-1}), and potential temperature ($^{\circ}\text{C}$; referenced to surface) as contours. Major currents are indicated: LC, Labrador Sea Boundary Current (BC), WGC, EGC, IC, and NAC.

Across the Labrador Sea (VITALS)] focused on carbon and oxygen cycles. VITALS will provide information on gas uptake and water mass formation north of the OSNAP West line, complementing the water mass information provided by the annual survey of the AR7W line (Yashayaev 2007).

Mooring arrays have been deployed at the continental boundaries and on the eastern and western flanks of the Reykjanes Ridge (Fig. 4). The OSNAP Reykjanes Ridge moorings are complemented by those from the French Reykjanes Ridge Experiments (RREX; Fig. 3c), an observational and modeling effort designed to study the processes controlling the dynamical connections between the two sides of the Reykjanes Ridge. Additional full-depth moorings containing temperature/salinity sensors have been placed at key locations to estimate geostrophic transports (Fig. 4). Additionally, in the eastern basin, a suite of gliders is measuring properties across the Rockall–Hatton Basin and westward into the Iceland Basin (Figs. 3a and 4b). Finally, acoustically tracked deep floats (RAFOS) have been released on the OSNAP lines to study the connectivity of overflow water pathways between moored arrays and to aid the interpretation of the Eulerian measurements (Fig. 3a).

The effectiveness of the proposed OSNAP design has been tested using a series of observing system simulation experiments (OSSEs) where basin-width integrated fluxes calculated from subsampled model fields are compared to the model “truth” or reference fluxes. OSNAP OSSEs were conducted using ORCA025, an intermediate resolution, or

eddy-permitting, configuration of the Nucleus for European Modelling of the Ocean (NEMO; Madec 2008). The OSSE mean overturning transports for 1990–2004 are within one standard deviation of the mean transports for the model truth, calculated over the same period: for OSNAP West the model truth mean transport in density space is $7.65 \pm 1.68 \text{ Sv}$ ($1 \text{ Sv} \equiv 10^6 \text{ m}^3 \text{ s}^{-1}$), while the OSSE mean transport is $7.78 \pm 1.73 \text{ Sv}$; for OSNAP East the model truth mean transport is $13.65 \pm 1.56 \text{ Sv}$, while the OSSE mean transport is $12.97 \pm 2.56 \text{ Sv}$. Furthermore, the proposed design does an impressive job of capturing the overturning variability, with a correlation of 0.89 (0.85) between the OSSE and the reference time series for OSNAP West (East). Comparisons of heat and freshwater fluxes are also favorable: for OSNAP West, the total heat flux is $0.10 \pm 0.02 \text{ PW}$ for both the model truth and the OSSE (correlation coefficient $R = 0.94$), and the total freshwater flux relative to the section mean salinity is $-0.17 \pm 0.04 \text{ Sv}$ for the OSSE and -0.16 ± 0.04 for the model truth ($R = 0.90$); for OSNAP East, the total heat flux is $0.36 \pm 0.04 \text{ PW}$ for the model truth and $0.33 \pm 0.05 \text{ PW}$ for the OSSE ($R = 0.83$), and the total freshwater flux relative to the section mean salinity is $-0.14 \pm 0.05 \text{ Sv}$ for both the model truth and the OSSE ($R = 0.98$). All correlation coefficients in parentheses above denote agreement between the model truth and the OSSE time series. Readers are referred to F. Li et al. (2017, manuscript submitted to *J. Atmos. Oceanic Technol.*) for details on the calculation methodology and for information on steps we are currently taking to improve our estimates.

PROGRESS TO DATE. Recovery of the suite of data necessary for the calculation of transbasin volume, heat, and freshwater fluxes was completed in September 2016. The first OSNAP time series of these variables are expected in the fall of 2017. In addition to these basin integral measures, OSNAP will produce, and indeed is already producing, observations of the circulation and property fields across the subpolar gyre. Data that have been collected to date, discussed below, reveal the rich spatial and temporal variability of those fields. The OSNAP observational program is complemented by modeling theoretical and data analyses efforts that aim to 1) place the observations in a broader spatial and temporal context and 2) link the observations to forcing mechanisms. Preliminary efforts toward this end are also discussed below. Please note that the sections below do not constitute a preliminary look at the comprehensive measurements

that will result from the entire suite of OSNAP data, namely, the volume, heat, and freshwater transports. Rather, the sections below illustrate the wide variety of investigations possible under OSNAP.

First look at the OSNAP cross-sectional velocity field.

The OSNAP line was first surveyed with a conductivity–temperature–depth (CTD) section in June–July 2014 on Royal Research Ship (RRS) *James Clark Ross*, providing the first modern, quasi-synoptic hydrographic and biogeochemical section from North America to Europe at subpolar latitudes [King and Holliday 2015; see Kieke and Yashayaev (2015) for a review of other hydrographic surveys in the subpolar basin]. The cross-sectional geostrophic velocity field from the survey illustrates the complexity of the circulation in this region [Fig. 5, derived from CTD profiles, the thermal wind equation, and a reference velocity from a lowered

acoustic Doppler current profiler (ADCP), following the method in Holliday et al. (2009)]. The warm North Atlantic Current (NAC) can be seen as two major shallow and surface-intensified currents in the Iceland Basin, plus a jet in the western Rockall Trough, and the cooler Irminger Current (IC) on the west side of the Reykjanes Ridge. Between the major currents there are transient eddies and more persistent topographically steered recirculation features. In the Irminger and Labrador Seas, the fast gyre boundary currents can be seen tight against the continental slopes of Greenland and Canada. In the western gyre, the boundary currents are deep-reaching features, linking the surface circulation to the cold, deep overflow waters (<3.0°C). In contrast, from the western side of the Reykjanes Ridge across to Rockall, the upper ocean is often moving in a direction opposite that of the deepest layers. In the

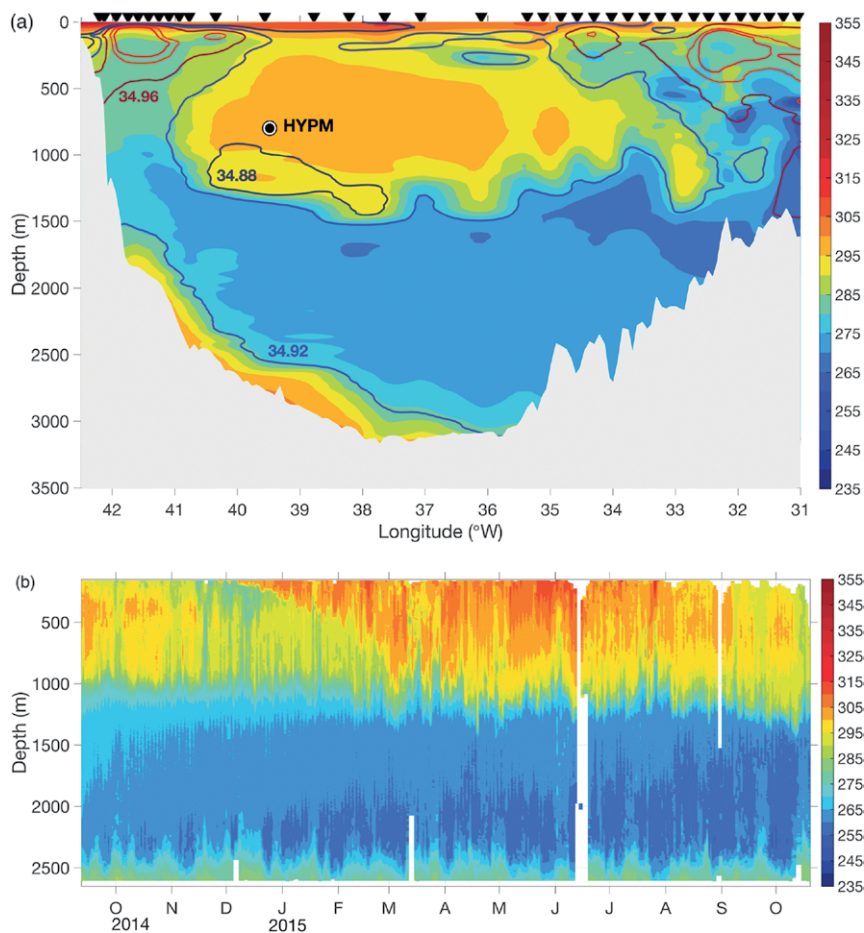


FIG. 6. (a) Hydrography in the Irminger Sea observed in Jul 2015. Dissolved oxygen values are plotted with color shading ($\mu\text{mol kg}^{-1}$). The colored lines are salinity contours plotted at 0.04 intervals. CTD station locations are indicated with triangles at the top. (b) Time series of dissolved oxygen ($\mu\text{mol kg}^{-1}$) from the OOI HYPM mooring, whose location is indicated with a black circle in (a). White areas denote missing data.

Iceland Basin, the multiple current cores of overflow waters lie under a thick layer of slowly circulating LSW and are also subject to recirculation (e.g., southward cores at ~2,300 and ~2,450 km, and recirculation at ~2,400 and ~2,600 km in Fig. 5). The OSNAP moorings and Lagrangian observations of overflow pathways will help put these synoptic observations into context and reveal variability on time scales shorter than the time it takes to complete a synoptic survey.

Hydrography across the Irminger and Labrador Seas: Signatures of strong convection. The deployment of the OSNAP array in the summer of 2014 was auspiciously timed, as revealed by a hydrographic survey along the OSNAP line in the Irminger Sea in the summer of 2015 (de Steur 2015). The survey revealed a large body of water with high dissolved oxygen content and low salinity that fills the central part of the basin at upper to intermediate depths (Fig. 6a). Year-round observations from a profiling mooring in the Irminger Gyre confirm that this water was formed locally in the strong winter of 2014/15, when mixed layer depths reached down to 1,400 m (de Jong and de Steur 2016). The first time series from the OOI Irminger Sea global node (Fig. 6b) shows the sharp increase in oxygen concentration as convection deepens the mixed layer from November to December. These observations confirm the role of the Irminger Sea as a convective basin in addition to the Labrador Sea, as suggested earlier by Pickart et al. (2003). In the Labrador Sea, strong convection also took place in the winter of 2014/15 (Yashayaev and Loder 2016). In addition to this signature of deep convection, the survey also shows the familiar features of the warm and saline Irminger Current on the eastern and western boundaries of the basin, as well as the cold, dense, and oxygen-rich DSWC carried along the East Greenland slope by the DWBC. A new feature, however, is the signature of stirring between the interior waters (high in oxygen) and boundary current water (low in oxygen) that appears over the western flank of the Mid-Atlantic Ridge. Interestingly, deep convection and enhanced mesoscale eddy exchange may well be related—a connection that will be investigated in detail with OSNAP data.

The evolution of convection in the Labrador Basin during the winter of 2014/15 will be further elucidated once data from the OSNAP West arrays (on a 2-yr schedule) are retrieved and processed. The analysis of that data will be advantaged by the fact that there have been sustained observations in the basin interior (see K1 in Fig. 3a) and in the

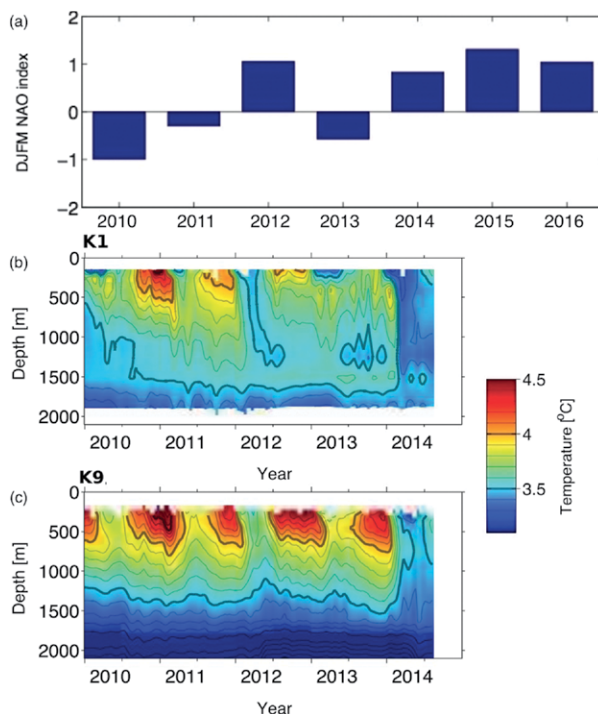


Fig. 7. (a) Winter [Dec–Mar (DJFM)] mean NAO index. Time series of temperature from the (b) K1 and (c) K9 moorings. The mooring locations are shown in Fig. 3a.

boundary current off the Labrador coast since 1997 (see the German boundary array in Fig. 3a; Fischer et al. 2004), well before the deployment of the OSNAP array in the summer of 2014. Observations from both sites allow for the study of how convectively transformed waters from the Labrador Sea are exported to the boundary current and for a study of water mass transformation within the boundary current itself. The simultaneous observations at K1 and K9 since 2009 have offered an interesting contrast. As seen in Fig. 7a, the 2013/14 winter was characterized by a positive North Atlantic Oscillation (NAO) index that has persisted to present (www.cpc.ncep.noaa.gov). An increase in surface buoyancy loss over the Labrador Sea during this positive NAO index period goes along with an abrupt change in mixed layer depths in excess of 1,500 m in the boundary current (at K9; see location in Fig. 3a) and in the central Labrador Sea (at K1), a situation last documented in the 2007/08 winter (Yashayaev and Loder 2009). While the 2013/14 response is similar at both sites (though stronger in the interior, at K1), the boundary current response to the 2011/12 NAO forcing is decidedly weaker. Though it has been pointed out that the NAO index does not optimally indicate buoyancy forcing changes in the Labrador Sea (e.g., Grist et al. 2016), these observations alone highlight the fact that the

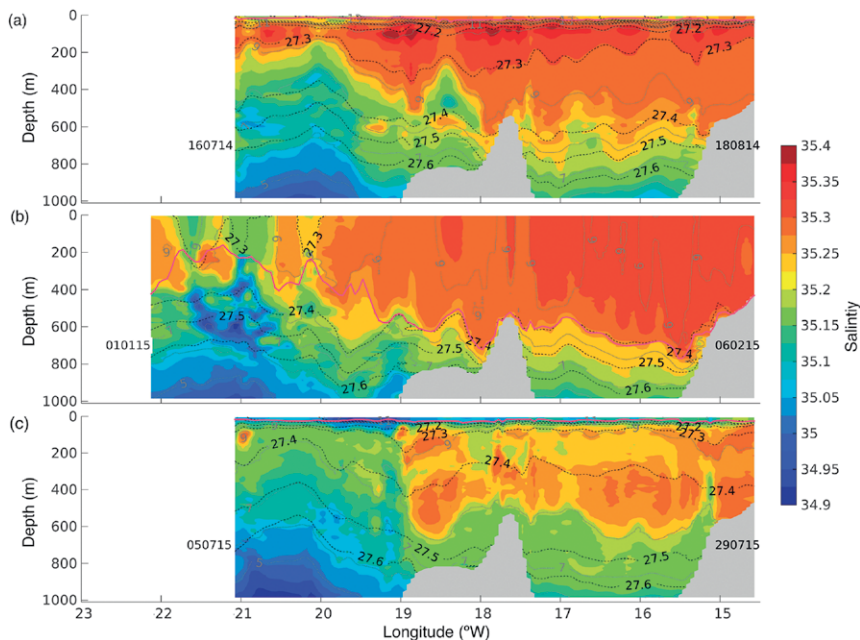


FIG. 8. Three glider sections on Rockall Plateau along 58°N in (a) Jul–Aug 2014, (b) Jan 2015, and (c) Jul 2015. Labels on the left and right sides of the sections indicate the date at the beginning and end of the section (ddmm-yy), respectively. Contours are of salinity (color), potential temperature (gray lines), and potential density (black dashed line) referenced to the surface. The mixed layer depth, calculated using a reference level at 10-m depth and a criterion $\Delta\sigma_\theta = 0.03 \text{ kg m}^{-3}$, is shown by the red line. The profile path taken by the glider is V shaped, with a typical horizontal separation of 2–6 km. Descent and ascent speeds are $\sim 10\text{--}20 \text{ cm s}^{-1}$ and forward speed is $\sim 20\text{--}40 \text{ cm s}^{-1}$. Vertical resolution of sampling is $\sim 0.5\text{--}1.5 \text{ m}$ above the main pycnocline and $\sim 1.5\text{--}3 \text{ m}$ below.

dynamical link between deep convection in the Labrador Sea and the export of newly formed deep waters in the boundary current remains unresolved. Results from the OSNAP array will enable an investigation of the link between deep mixing, the net water mass formation, and the dynamics of the export.

Glider observations in the eastern subpolar region. Some areas across the OSNAP line have been monitored or at least intermittently measured for years, for example, the waters of the DWBC off the Labrador coast. However, in other areas there are only sparse historical observations, particularly of the flow field, a prime example of which is the Rockall Plateau. Though these observations have been too few to estimate the circulation in this region, ocean model simulations indicate that 2–5 Sv of northward flow should be found here, a sizeable contribution to the total northward flow across the OSNAP East line. However, because the plateau is shallow, no Argo floats are deployed across or drift over the plateau, and because of fishing activities moorings are unlikely to survive.

Thus, gliders were chosen to provide property, transport, and flux measurements across the plateau. Ten OSNAP glider sections were realized between 21° and 15°W from July 2014 to November 2015 of which three are shown in Fig. 8. Data from past glider missions and real-time data from current missions may be viewed online (<http://velocity.sams.ac.uk/gliders/>).

A remarkable feature of these measurements is the signature of intense vertical mixing that occurred in the 2014/15 winter. This mixing deepened the mixed layer to 700 m (Fig. 8b) and resulted in the formation of anomalously large volumes of Subpolar Mode Water (SPMW) in the density range $\sigma_\theta = 27.3\text{--}27.4$. In a recent paper, Grist et al. (2016) show how excess formation of SPMW in winter (2013/14) relates to extreme North American tempera-

tures and record-breaking precipitation over the United Kingdom during that winter. This volume of SPMW in the density range of $\sigma_\theta = 27.3\text{--}27.4$ is capped by seasonal stratification (Fig. 8a). In the following winter of 2014/15 (Fig. 8b), intense vertical mixing deepens the mixed layer to 700 m. By the following summer (Fig. 8c), the SPMW is again capped by seasonal stratification and there is a larger, denser volume of SPMW than the previous year. These first observations confirm that the OSNAP glider across the Rockall Plateau is well placed to observe the evolution of SPMW and to quantify ocean–atmosphere dynamic exchanges.

Gliders are also being employed to enhance the OSNAP data coverage in the eddy-rich region of the Iceland Basin where the NAC flows northward across the section, often in multiple branches (Fig. 5). One glider, deployed on the OSNAP East line in June 2015 and recovered in November 2015, accomplished 519 profiles with a depth range between 0 and 1,000 m while patrolling between moorings M3 and M4 (green line, Fig. 3a). Over this time period, the

glider sampled a strong anticyclonic eddy between the M3 and M4 moorings (Fig. 9). An anticyclonic eddy is often present in this region, and it is a feature of the long-term (20 yr) mean absolute dynamic topography [ADT; the altimeter ADT products were produced by Segment Sol multimissions d'ALTimétrie, d'Orbitographie et de localisation précise (SSALTO)/Data Unification and Altimeter Combination System (DUACS) and distributed by Archiving, Validation, and Interpretation of Satellite Oceanographic Data (AVISO), with support from the Centre National d'Études Spatiales (CNES; AVISO 2016)]. Despite rotational currents that affected its path, the glider successfully produced a hydrographic section that shows relatively warm, salty, and high-oxygen waters for the eddy core, indicating that the water trapped in the eddy is probably recently ventilated water from the NAC. The eddy moved northeastward by the time of the second glider deployment, revealing the relatively smooth front separating the warm, salty, and low-oxygen water in the east from the relatively cold, fresh, and high-oxygen water in the west. The high-resolution sections of temperature, salinity, and geostrophic velocity across this region provided by the gliders will lead to increased accuracy in estimates of heat and freshwater flux over that available from the mooring observations and Argo data alone.

Complementary model- and data-based analyses. To quantify the transformation of the warm waters of the AMOC upper limb that flow northward across the OSNAP line into cooler waters that return southward at depth across the line, information is needed on the surface fluxes of heat and freshwater responsible for the transformation. A regional thermohaline inverse method (RTHIM) that extends the Walin (1982) water mass transformation framework to two water mass coordinates (Groeskamp et al. 2014) quantifies this transformation using surface fluxes from climate reanalysis and observations from Argo floats and satellite altimetry. Importantly, RTHIM provides an estimate of the volume fluxes (AMOC) independent of the OSNAP array observations. RTHIM has been successfully validated against a numerical simulation of the subpolar/Arctic region using a 1° ORCA model. Further validation, including more realistic boundary currents and mesoscale eddies, is underway. The method's strength is that it allows for a determination of the relative importance of interior mixing and surface fluxes to the transformation of water masses in the subpolar/Arctic region. Given that surface flux observations in the Arctic are sparse, we plan to use several reanalysis products, recently evaluated in

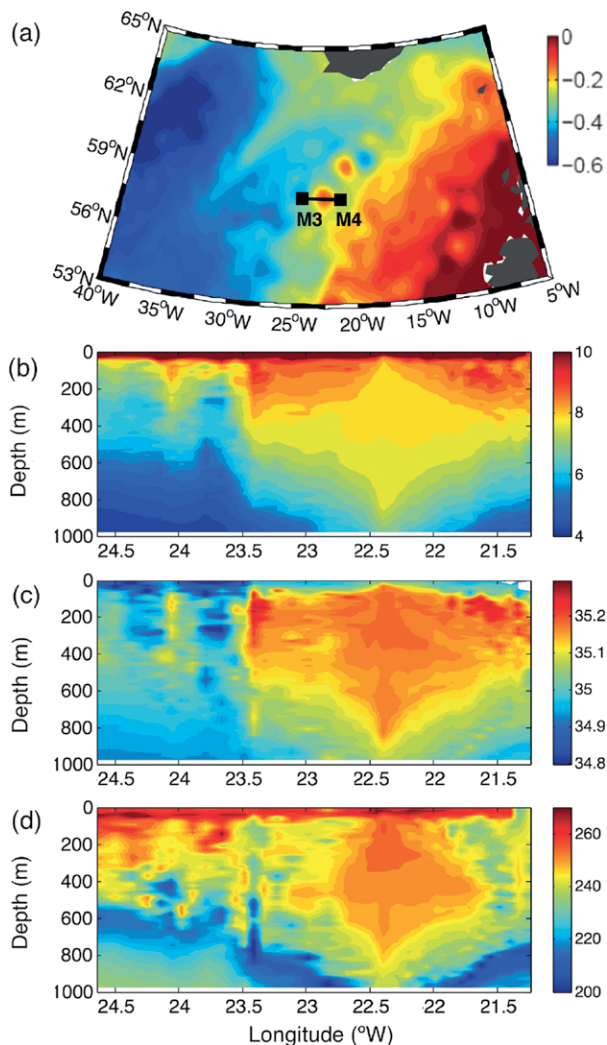


FIG. 9. (a) ADT (m) between 23 Jul and 2 Aug 2015, showing an anticyclonic eddy on the OSNAP line. The two black squares denote moorings M3 and M4, and a black line represents the sampling path. (b) Temperature (°C), (c) salinity, and (d) dissolved oxygen ($\mu\text{mol kg}^{-1}$) data recorded by the glider during the eddy scenario are shown.

Lindsay et al. (2014), to derive a set of RTHIM solutions and uncertainties. When applied to the observations, this technique will provide a proxy measure of the AMOC over the time span leading up to OSNAP, helping us place the variability observed by the array in a broader temporal context.

To better understand, and ultimately predict, inter-annual and decadal variability in the AMOC, a quantification of its sensitivity to changes in surface forcing is needed. This quantification is most efficiently accomplished using an adjoint modeling approach that provides the linear sensitivity of the AMOC at a single latitude to changes in surface forcing over the globe, for all forcing lead times (Pillar et al. 2016). Sensitivity

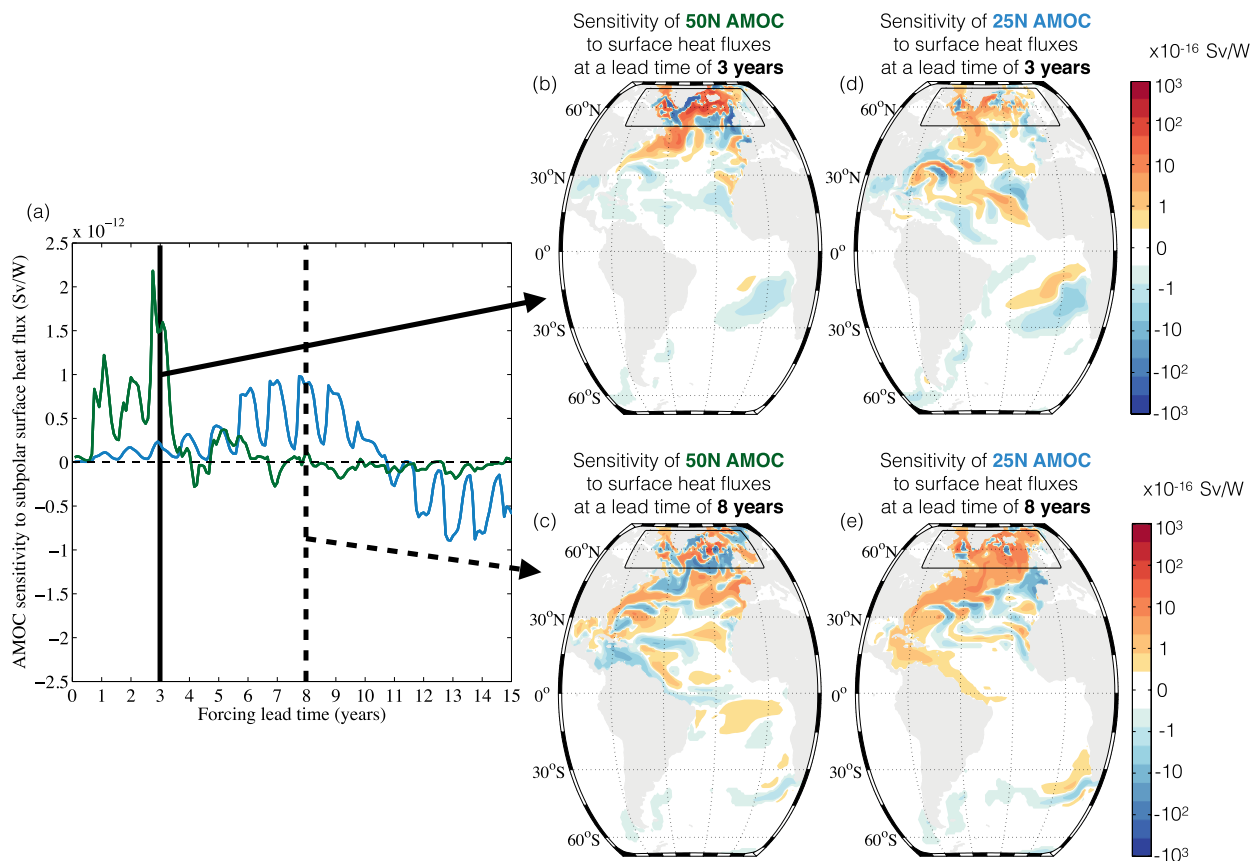


FIG. 10. Linear sensitivity of the AMOC at (d), (e) 25°N and (b), (c) 50°N in Jan to surface heat flux anomalies per unit area. Positive sensitivity indicates that ocean cooling leads to an increased AMOC—e.g., in the upper panels, a unit increase in heat flux out of the ocean at a given location will change the AMOC at (d) 25°N or (e) 50°N 3 yr later by the amount shown in the color bar. The contour intervals are logarithmic. (a) The time series show linear sensitivity of the AMOC at 25°N (blue) and 50°N (green) to heat fluxes integrated over the subpolar gyre (black box with surface area of $\sim 6.7 \times 10^6 \text{ m}^2$) as a function of forcing lead time. The reader is referred to Pillar et al. (2016) for model details and to Heimbach et al. (2011) and Pillar et al. (2016) for a full description of the methodology and discussion relating to the dynamical interpretation of the sensitivity distributions.

distributions of the AMOC at 25° and 50°N to surface heat flux anomalies throughout the Atlantic basin are compared in Figs. 10b–e for forcing at lead times of 3 and 8 yr. Differences in these sensitivity distributions indicate key regions and lead times at which surface heat flux anomalies may force a notable deviation between the response of the AMOC observed at the RAPID–MOCHA and OSNAP monitoring arrays.

To further illustrate this point, we show the sensitivity of the AMOC at 25°N (blue) and 50°N (green) to surface heat flux anomalies integrated over the subpolar gyre, as a function of forcing lead time (up to 15 yr), in Fig. 10a. Examination of this spatially integrated sensitivity is useful for approximating the AMOC response to regional heat flux anomalies of the same sign, such as those associated with the NAO (e.g., Eden and Jung 2001). At 25°N, the AMOC response to NAO-type heat fluxes over the subpolar gyre oscillates in sign on decadal time scales (Czeschel et al. 2010). In contrast, at

50°N, the AMOC response to the same forcing notably diminishes for forcing lead times exceeding 5 yr, due to a large cancellation in the integral associated with smaller-scale structures in the sensitivity distributions (Fig. 10c). These results highlight the need to further explore the full spatial structure of AMOC sensitivity and better constrain variations in surface buoyancy forcing, supporting the expectation that subpolar monitoring under OSNAP will be invaluable in helping us to understand—and possibly predict—low-frequency variability in the AMOC at the RAPID–MOCHA.

ANTICIPATED OSNAP DATA PRODUCTS AND TIMELINE. OSNAP data products will parallel those of the RAPID–MOCHA program, namely, time series of the overturning circulation, and the depth and zonally integrated heat and freshwater fluxes. The OSNAP overturning metric will be reported in both depth and density coordinates.

The OSNAP principal investigators (PIs) are committed to timely delivery of OSNAP products. The earliest expected delivery of the first OSNAP products is one year following the retrieval of all data necessary for the calculations, that is, early fall of 2017 (see www.o-snap.org for further information on OSNAP, including cruise reports, blogs, and technical information on all OSNAP arrays).

SUMMARY. For decades oceanographers have assumed the AMOC to be highly susceptible to changes in the production of deep waters at high latitudes in the North Atlantic. A new ocean observing system is now in place that will test that assumption. Early results from the OSNAP observational program reveal the complexity of the velocity field across the section and the dramatic increase in convective activity during the 2014/15 winter. Early results from the gliders that survey the eastern portion of the OSNAP line have illustrated the importance of these measurements for estimating meridional heat fluxes and for studying the evolution of Subpolar Mode Waters. Finally, numerical modeling data have been used to demonstrate the efficacy of a proxy AMOC measure based on a broader set of observational data, and an adjoint modeling approach has shown that measurements in the OSNAP region will aid our mechanistic understanding of the low-frequency variability of the AMOC in the subtropical North Atlantic.

Finally, we note that while a primary motivation for studying AMOC variability comes from its potential impact on the climate system, as mentioned above, additional motivation for the measure of the heat, mass, and freshwater fluxes in the subpolar North Atlantic arises from their potential impact on marine biogeochemistry and the cryosphere. Thus, we hope that this observing system can serve the interests of the broader climate community.

ACKNOWLEDGMENTS. The authors gratefully acknowledge financial support from the U.S. National Science Foundation (NSF; OCE-1259102, OCE-1259103, OCE-1259618, OCE-1258823, OCE-1259210, OCE-1259398, OCE-0136215, and OCE-1005697); the U.S. National Aeronautics and Space Administration (NASA); the U.S. National Oceanic and Atmospheric Administration (NOAA); the WHOI Ocean and Climate Change Institute (OCCI), the WHOI Independent Research and Development (IRD) Program, and the WHOI Postdoctoral Scholar Program; the U.K. Natural Environment Research Council (NERC; NE/K010875/1, NE/K010700/1, R8-H12-85, FASTNEt NE/I030224/1, NE/K010972/1, NE/K012932/1, and NE/M018024/1); the European Union Seventh Framework Programme (NACLIM

project, 308299 and 610055); the German Federal Ministry and Education German Research RACE Program; the Natural Sciences and Engineering Research Council of Canada (NSERC; RGPIN 227438-09, RGPIN 04357, and RG-PCC 433898); Fisheries and Oceans Canada; the National Natural Science Foundation of China (NSFC; 41521091, U1406401); the Fundamental Research Funds for the Central Universities of China; the French Research Institute for Exploitation of the Sea (IFREMER); the French National Center for Scientific Research (CNRS); the French National Institute for Earth Sciences and Astronomy (INSU); the French national program LEFE; and the French Oceanographic Fleet (TGIR FOF).

REFERENCES

- AVISO, 2016: Ssalto/Duacs multimission altimeter products. [Available online at www.aviso.altimetry.fr/duacs/.]
- Baehr, J., A. Stroup, and J. Marotzke, 2009: Testing concepts for continuous monitoring of the meridional overturning circulation in the South Atlantic. *Ocean Modell.*, **29**, 147–153, doi:10.1016/j.ocemod.2009.03.005.
- Bingham, R. J., C. W. Hughes, V. Roussenov, and R. G. Williams, 2007: Meridional coherence of the North Atlantic meridional overturning circulation. *Geophys. Res. Lett.*, **34**, L23606, doi:10.1029/2007GL031731.
- Bower, A. S., M. S. Lozier, S. F. Gary, and C. Böning, 2009: Interior pathways of the Atlantic meridional overturning circulation. *Nature*, **459**, 243–247, doi:10.1038/nature07979.
- Buckley, M., and J. Marshall, 2016: Observations, inferences, and mechanisms of the Atlantic Meridional Overturning Circulation: A review. *Rev. Geophys.*, **54**, doi:10.1002/2015RG000493.
- Clarke, R. A., R. M. Hendry, and I. Yashayaev, 1998: A western boundary current meter array in the North Atlantic near 42°N. *International WOCE Newsletter*, No. 33, WOCE International Project Office, Southampton, United Kingdom, 33–34.
- Condrón, A., and P. Winsor, 2011: A subtropical fate awaited freshwater discharged from glacial Lake Agassiz. *Geophys. Res. Lett.*, **38**, L03705, doi:10.1029/2010GL046011.
- Cunningham, S., and R. Marsh, 2010: Observing and modeling changes in the Atlantic MOC. *Wiley Interdiscip. Rev.: Climate Change*, **1**, 180–191, doi:10.1002/wcc.22.
- , and Coauthors, 2007: Temporal variability of the Atlantic meridional overturning circulation at 25°N. *Science*, **317**, 935–938, doi:10.1126/science.1141304.
- , and Coauthors, 2010: The present and future system for measuring the Atlantic Meridional Overturning

- Circulation and heat transport. *Proceedings of OceanObs'09: Sustained Ocean Observations and Information for Society*, J. Hall, D. E. Harrison, and D. Stammer, Eds., ESA Publ. WPP-306, doi:10.5270/OceanObs09.cwp.21.
- Czeschel, L., D. P. Marshall, and H. L. Johnson, 2010: Oscillatory sensitivity of Atlantic overturning to high-latitude forcing. *Geophys. Res. Lett.*, **37**, L10601, doi:10.1029/2010GL043177.
- Danabasoglu, G., and Coauthors, 2016: North Atlantic simulations in Coordinated Ocean-ice Reference Experiments phase II (CORE-II). Part II: Interannual to decadal variability. *Ocean Modell.*, **97**, 65–90, doi:10.1016/j.ocemod.2015.11.007.
- de Jong, M. F., and L. de Steur, 2016: Strong winter cooling over the Irminger Sea in winter 2014–2015, exceptional deep convection, and the emergence of anomalously low SST. *Geophys. Res. Lett.*, **43**, 7106–7113, doi:10.1002/2016GL069596.
- Delworth, T. L., R. Zhang, and M. E. Mann, 2007: Decadal to centennial variability of the Atlantic from observations and models. *Ocean Circulation: Mechanisms and Impacts—Past and Future Changes of Meridional Overturning*, *Geophys. Monogr.*, Vol. 173, Amer. Geophys. Union, 131–148, doi:10.1029/173GM10.
- Dengler, M., J. Fischer, F. A. Schott, and R. Zantopp, 2006: Deep Labrador Current and its variability in 1996–2005. *Geophys. Res. Lett.*, **33**, L21S06, doi:10.1029/2006GL026702.
- Deshayes, J., F. Straneo, and M. A. Spall, 2009: Mechanisms of variability in a convection basin. *J. Mar. Res.*, **67**, 273–303, doi:10.1357/002224009789954757.
- de Steur, L., 2015: Cruise report: Cruise 64PE400; OS-NAP East leg 2, July 8–29 2015, Reykjavik-Reykjavik, Iceland, R/V Pelagia. Royal Netherlands Institute for Sea Research, 48 pp. [Available online at www.vliz.be/nl/imis?module=ref&refid=260561&printversion=1&dropIMISitle=1.]
- Eden, C., and T. Jung, 2001: North Atlantic interdecadal variability: Oceanic response to the North Atlantic oscillation (1865–1997). *J. Climate*, **14**, 676–691, doi:10.1175/1520-0442(2001)014<0676:NAIVOR>2.0.CO;2.
- Fischer, J., F. Schott, and M. Dengler, 2004: Boundary circulation at the exit of the Labrador Sea. *J. Phys. Oceanogr.*, **34**, 1548–1570, doi:10.1175/1520-0485(2004)034<1548:BCATEO>2.0.CO;2.
- Grist, J. P., S. A. Josey, Z. L. Jacobs, R. Marsh, B. Sinha, and E. Van Sebille, 2016: Extreme air–sea interaction over the North Atlantic subpolar gyre during the winter of 2013–2014 and its sub-surface legacy. *Climate Dyn.*, **46**, 4027, doi:10.1007/s00382-015-2819-3.
- Groeskamp, S., J. D. Zika, B. M. Sloyan, T. J. McDougall, and P. C. McIntosh, 2014: A thermohaline inverse method for estimating diathermohaline circulation and mixing. *J. Phys. Oceanogr.*, **44**, 2681–2697, doi:10.1175/JPO-D-14-0039.1.
- Halloran, P. R., B. B. Booth, C. D. Jones, F. H. Lambert, D. J. McNeill, I. J. Totterdell, and C. Völker, 2015: The mechanisms of North Atlantic CO₂ uptake in a large Earth System Model ensemble. *Biogeosciences*, **12**, 4497–4508, doi:10.5194/bgd-11-14551-2014.
- Hansen, B., and S. Østerhus, 2007: Faroe Bank Channel overflow 1995–2005. *Prog. Oceanogr.*, **75**, 817–856, doi:10.1016/j.pocean.2007.09.004.
- Heimbach, P., C. Wunsch, R. Ponte, G. Forget, C. Hill, and J. Utke, 2011: Timescales and regions of the sensitivity of Atlantic meridional volume and heat transport: Toward observing system design. *Deep-Sea Res. II*, **58**, 1858–1879, doi:10.1016/j.dsr2.2010.10.065.
- Hirschi, J., and J. Marotzke, 2007: Reconstructing the meridional overturning circulation from boundary densities and the zonal wind stress. *J. Phys. Oceanogr.*, **37**, 743–763, doi:10.1175/JPO3019.1.
- Holland, D. M., R. H. Thomas, B. deYoung, M. H. Ribergaard, and B. Lyberth, 2008: Acceleration of Jakobshavn Isbræ triggered by warm subsurface ocean waters. *Nat. Geosci.*, **1**, 659–664, doi:10.1038/ngeo316.
- Holliday, N. P., S. Bacon, J. Allen, and E. L. McDonagh, 2009: Circulation and transport in the western boundary current at Cape Farewell, Greenland. *J. Phys. Oceanogr.*, **39**, 1854–1870, doi:10.1175/2009JPO4160.1.
- , S. A. Cunningham, C. Johnson, S. Gary, C. Griffiths, J. F. Read, and T. Sherwin, 2015: Multidecadal variability of potential temperature, salinity and transport in the eastern subpolar North Atlantic. *J. Geophys. Res. Oceans*, **120**, 5945–5967, doi:10.1002/2015JC010762.
- IPCC, 2013: *Climate Change 2013: The Physical Science Basis*. Cambridge University Press, 1535 pp., doi:10.1017/CBO9781107415324.
- Jackson, L., R. Kahana, T. Graham, M. Ringer, T. Woollings, J. Mecking, and R. Wood, 2015: Global and European climate impacts of a slowdown of the AMOC in a high resolution GCM. *Climate Dyn.*, **45**, 3299–3316, doi:10.1007/s00382-015-2540-2.
- Jochumsen, K., D. Quadfasel, H. Valdimarsson, and S. Jónsson, 2012: Variability of the Denmark Strait overflow: Moored time series from 1996–2011. *J. Geophys. Res.*, **117**, C12003, doi:10.1029/2012JC008244.
- Kanzow, T., and Coauthors, 2007: Flow compensation associated with the MOC at 26.5°N in the Atlantic. *Science*, **317**, 938–941, doi:10.1126/science.1141293.
- Karspeck, A. R., and Coauthors, 2015: Comparison of the Atlantic meridional overturning circulation

- between 1960 and 2007 in six ocean reanalysis products. *Climate Dyn.*, doi:10.1007/s00382-015-2787-7, in press.
- Khatiwala, S., and Coauthors, 2013: Global ocean storage of anthropogenic carbon. *Biogeosciences*, **10**, 2169–2191, doi:10.5194/bg-10-2169-2013.
- Kieke, D., and I. Yashayaev, 2015: Studies of Labrador Sea water formation and variability in the subpolar North Atlantic in the light of international partnership and collaboration. *Prog. Oceanogr.*, **132**, 220–232, doi:10.1016/j.pocean.2014.12.010.
- King, B. A., and N. P. Holliday, 2015: RRS *James Clark Ross* cruise 302, 06 Jun–21 Jul 2014: The 2015 RAG-NARRoC, OSNAP and extended Ellett Line cruise report. National Oceanography Centre Cruise Rep. 35, 76 pp.
- Knight, J. R., R. J. Allan, C. K. Folland, M. Vellinga, and M. E. Mann, 2005: A signature of persistent natural thermohaline circulation cycles in observed climate. *Geophys. Res. Lett.*, **32**, L20708, doi:10.1029/2005GL024233.
- , C. K. Folland, and A. A. Scaife, 2006: Climatic impacts of the Atlantic multidecadal oscillation. *Geophys. Res. Lett.*, **33**, L17706, doi:10.1029/2006GL026242.
- Kortzinger, A., U. Send, D. W. R. Wallace, J. Karstensen, and M. DeGrandpre, 2008: The seasonal cycle of O₂ and pCO₂ in the central Labrador Sea: Atmospheric, biological and physical implications. *Global Biogeochem. Cycles*, **22**, doi:10.1029/2007GB003029.
- Kuhlbrodt, T., A. Griesel, M. Montoya, A. Levermann, M. Hofmann, and S. Rahmstorf, 2007: On the driving processes of Atlantic meridional overturning circulation. *Rev. Geophys.*, **45**, 32, doi:10.1029/2004RG000166.
- Lazier, J., R. Hendry, A. Clarke, I. Yashayaev, and P. Rhines, 2002: Convection and restratification in the Labrador Sea, 1990–2000. *Deep-Sea Res. I*, **49**, 1819–1835, doi:10.1016/S0967-0637(02)00064-X.
- Li, H., T. Ilyina, A. Wolfgang, A. Müller, and F. Sienz, 2016: Decadal predictions of the North Atlantic CO₂ uptake. *Nat. Commun.*, **7**, 11076, doi:10.1038/ncomms11076.
- Lindsay, R., M. Wensnahan, and A. Schweiger, 2014: Evaluation of seven different atmospheric reanalysis products in the Arctic. *J. Climate*, **27**, 2588–2606, doi:10.1175/JCLI-D-13-00014.1.
- Lozier, M. S., 2012: Overturning in the North Atlantic. *Annu. Rev. Mar. Sci.*, **4**, 291–315, doi:10.1146/annurev-marine-120710-100740.
- , S. F. Gary, and A. S. Bower, 2013: Simulated pathways of the overflow waters in the North Atlantic: Subpolar to subtropical export. *Deep-Sea Res. II*, **85**, 147–153, doi:10.1016/j.dsr2.2012.07.037.
- Madec, G., 2008: NEMO ocean engine, version 3.0. IPSL Note du Pôle de modélisation 27, 209 pp.
- McCarthy, G. D., and Coauthors, 2015: Measuring the Atlantic Meridional Overturning Circulation at 26°N. *Prog. Oceanogr.*, **130**, 91–111, doi:10.1016/j.pocean.2014.10.006.
- Meinen, C. S., D. R. Watts, and R. A. Clarke, 2000: Absolutely referenced geostrophic velocity and transport on a section across the North Atlantic Current. *Deep-Sea Res. I*, **47**, 309–322, doi:10.1016/S0967-0637(99)00061-8.
- Mercier, H., and Coauthors, 2015: Variability of the meridional overturning circulation at the Greenland–Portugal OVIDE section from 1993 to 2010. *Prog. Oceanogr.*, **132**, 250–261, doi:10.1016/j.pocean.2013.11.001.
- Palter, J. B., and M. S. Lozier, 2008: On the source of Gulf Stream nutrients. *J. Geophys. Res.*, **113**, C06018, doi:10.1029/2007JC004611.
- Pérez, F. F., H. Mercier, M. Vázquez-Rodríguez, P. Lherminier, A. Velo, P. Pardo, G. Roson, and A. Rios, 2013: Atlantic Ocean CO₂ uptake reduced by weakening of the meridional overturning circulation. *Nat. Geosci.*, **6**, 146–152, doi:10.1038/ngeo1680.
- Pickart, R. S., T. K. McKee, D. J. Torres, and S. A. Harrington, 1999: Mean structure and interannual variability of the slope water system south of Newfoundland. *J. Phys. Oceanogr.*, **29**, 2541–3132, doi:10.1175/1520-0485(1999)029<2541:MSAIVO>2.0.CO;2.
- , F. Straneo, and G. W. K. Moore, 2003: Is Labrador Sea Water formed in the Irminger Basin? *Deep-Sea Res. I*, **50**, 23–52, doi:10.1016/S0967-0637(02)00134-6.
- Pillar, H., P. Heimbach, H. Johnson, and D. Marshall, 2016: Dynamical attribution of recent variability in Atlantic overturning. *J. Climate*, **29**, 3339–3352, doi:10.1175/JCLI-D-15-0727.1.
- Rhines, P., S. Häkkinen, and S. A. Josey, 2008: Is oceanic heat transport significant in the climate system? *Arctic-Subarctic Ocean Fluxes: Defining the Role of the Northern Seas in Climate*, R. R. Dickson, J. Meincke, and P. Rhines, Eds., Springer, 87–109, doi:10.1007/978-1-4020-6774-7_5.
- Rignot, E., and P. Kanagaratnam, 2006: Changes in the velocity structure of the Greenland Ice Sheet. *Science*, **311**, 986–990, doi:10.1126/science.1121381.
- Robson, J. I., R. Sutton, K. Lohmann, and D. Smith, 2012: Causes of the rapid warming of the North Atlantic Ocean in the mid-1990s. *J. Climate*, **25**, 4116–4134, doi:10.1175/JCLI-D-11-00443.1.
- Rosón, G., A. F. Ríos, F. F. Pérez, A. Lavín, and H. L. Bryden, 2003: Carbon distribution, fluxes, and budgets in the subtropical North Atlantic Ocean (24.5°N). *J. Geophys. Res.*, **108**, 3144, doi:10.1029/1999JC000047.

- Sabine, C. L., and Coauthors, 2004: The oceanic sink for anthropogenic CO₂. *Science*, **305**, 367–371, doi:10.1126/science.1097403.
- Schott, F. A., J. Fischer, M. Dengler, and R. Zantopp, 2006: Variability of the Deep Western Boundary Current east of the Grand Banks. *Geophys. Res. Lett.*, **33**, L21S07, doi:10.1029/2006GL026563.
- Send, U., and J. Marshall, 1995: Integral effects of deep convection. *J. Phys. Oceanogr.*, **25**, 855–872, doi:10.1175/1520-0485(1995)025<0855:IEODC>2.0.CO;2.
- Serreze, M. C., M. M. Holland, and J. Stroeve, 2007: Perspectives on the Arctic's shrinking sea-ice cover. *Science*, **315**, 1533–1536, doi:10.1126/science.1139426.
- Smith, D. M., R. Eade, N. J. Dunstone, D. Fereday, J. M. Murphy, H. Pohlmann, and A. A. Scaife, 2010: Skilful multi-year predictions of Atlantic hurricane frequency. *Nat. Geosci.*, **3**, 846–849, doi:10.1038/ngeo1004.
- Spall, M. A., 2004: Boundary currents and water mass transformation in marginal seas. *J. Phys. Oceanogr.*, **34**, 1197–1213, doi:10.1175/1520-0485(2004)034<1197:BCAWTI>2.0.CO;2.
- , and R. S. Pickart, 2001: Where does dense water sink? A subpolar gyre example. *J. Phys. Oceanogr.*, **31**, 810–826, doi:10.1175/1520-0485(2001)031<0810:WD DWSA>2.0.CO;2.
- Steinfeldt, R., M. Rhein, J. L. Bullister, and T. Tanhua, 2009: Inventory changes in anthropogenic carbon from 1997–2003 in the Atlantic Ocean between 20°S and 65°N. *Global Biogeochem. Cycles*, **23**, GB3010, doi:10.1029/2008GB003311.
- Stouffer, R. J., and Coauthors, 2006: Investigating the causes of the response of the thermohaline circulation to past and future climate changes. *J. Climate*, **19**, 1365–1387, doi:10.1175/JCLI3689.1.
- Stramma, L., D. Kieke, M. Rhein, F. Schott, I. Yashayaev, and K. P. Koltermann, 2004: Deep water changes at the western boundary of the subpolar North Atlantic during 1996 to 2001. *Deep-Sea Res. I*, **51**, 1033–1056, doi:10.1016/j.dsr.2004.04.001.
- Straneo, F., 2006: Heat and freshwater transport through the central Labrador Sea. *J. Phys. Oceanogr.*, **36**, 606–628, doi:10.1175/JPO2875.1.
- , and P. Heimbach, 2013: North Atlantic warming and the retreat of Greenland's outlet glaciers. *Nature*, **504**, 36–43, doi:10.1038/nature12854.
- , G. S. Hamilton, D. A. Sutherland, L. A. Stearns, F. Davidson, M. O. Hammill, G. B. Stenson, and A. Rosing-Asvid, 2010: Rapid circulation of warm subtropical waters in a major glacial fjord off East Greenland. *Nat. Geosci.*, **3**, 182–186, doi:10.1038/ngeo764.
- Sutton, R. T., and D. L. R. Hodson, 2005: Atlantic Ocean forcing of North American and European summer climate. *Science*, **309**, 115–118, doi:10.1126/science.1109496.
- Takahashi, T., and Coauthors, 2009: Climatological mean and decadal change in surface ocean pCO₂, and net sea–air CO₂ flux over the global oceans. *Deep-Sea Res. II*, **56**, 554–577, doi:10.1016/j.dsr2.2008.12.009.
- U.S. CLIVAR AMOC Planning Team, 2007: Implementation strategy for a JSOST near-term priority assessing meridional overturning circulation variability: Implications for rapid climate change. U.S. CLIVAR Rep. 2007-2, 23 pp.
- Visbeck, M., 2007: Oceanography: Power of pull. *Nature*, **447**, 383, doi:10.1038/447383a.
- Walín, G., 1982: On the relation between sea-surface heat flow and thermal circulation in the ocean. *Tellus*, **34A**, 187–195, doi:10.1111/j.2153-3490.1982.tb01806.x.
- Xu, X., W. J. Schmitz, H. E. Hurlburt, P. J. Hogan, and E. P. Chassignet, 2010: Transport of Nordic Seas overflow water into and within the Irminger Sea: An eddy-resolving simulation and observations. *J. Geophys. Res.*, **115**, C12048, doi:10.1029/2010JC006351.
- Yashayaev, I., 2007: Hydrographic changes in the Labrador Sea, 1960–2005. *Prog. Oceanogr.*, **73**, 242–276, doi:10.1016/j.pocean.2007.04.015.
- , and J. W. Loder, 2009: Enhanced production of Labrador Sea Water in 2008. *Geophys. Res. Lett.*, **36**, L01606, doi:10.1029/2008GL036162.
- , and —, 2016: Recurrent replenishment of Labrador Sea Water and associated decadal-scale variability. *J. Geophys. Res. Oceans*, **121**, 8095–8114, doi:10.1002/2016JC012046.
- Yeager, S. G., A. Karspeck, G. Danabasoglu, J. Tribbia, and H. Teng, 2012: A decadal prediction case study: Late twentieth-century North Atlantic Ocean heat content. *J. Climate*, **25**, 5173–5189, doi:10.1175/JCLI-D-11-00595.1.
- Zhang, R., and T. L. Delworth, 2006: Impact of Atlantic multidecadal oscillations on India/Sahel rainfall and Atlantic hurricanes. *Geophys. Res. Lett.*, **33**, L17712, doi:10.1029/2006GL026267.
- Zou, S., and M. S. Lozier, 2016: Breaking the linkage between Labrador Sea Water production and its export to the subtropical gyre. *J. Phys. Oceanogr.*, **46**, 2169–2182, doi:10.1175/JPO-D-15-0210.1.
- Zweng, M. M., and Coauthors, 2013: *Salinity*. Vol. 2, *World Ocean Atlas 2013*, NOAA Atlas NESDIS 74, 39 pp.